Tuning the Spin Dynamics of Single Molecule Magnets via Dipolar Interactions

A Hofmann and Z Salman

Laboratory for Muon Spin Spectroscopy, Paul Scherrer Institute, CH-5232 Villigen PSI, Switzerland

Abstract. We present calculations of the dipolar field distribution acting on a single molecule magnet due to its neighbours in thin films. The calculations are presented for different packing/configuration scenarios, with different easy axis orientations. The potential for controlling the molecular spin dynamics by tuning the molecule-substrate interaction and its competition with intra-molecular interactions is discussed. We argue that by altering the configuration of the molecule moments, and thus their dipolar interactions, one can enhance or slow down their spin dynamics.

1. Introduction

Single molecule magnets (SMMs) [1] have attracted considerable attention in the last decade due to their fascinating magnetic properties [1, 2, 3]. They have also been considered for applications in quantum information processing [4, 5, 6]. As a result, a considerable focus in this field has shifted to the production and engineering of nano-structures of SMMs, e.g. deposition of thin films and monolayers on different substrates [7, 8, 9, 10, 11, 12, 13, 14, 15, 16, 17, 18]. New and novel techniques have proven successful for characterizing the magnetic properties of SMMs in these nano-structures [11, 12, 18, 19]. Depending on the type of studied SMM, some reports show that the bulk magnetic properties may be altered in a thin film or a monolayer due to its intra-molecular or molecule-substrate interactions. However, these studies have mostly focused on the static magnetic and low temperature properties of SMMs. Recent developments in low energy muon spin relaxation (LE-μSR)[20, 21] provide the possibility for depth-resolved [22] investigations of magnetic properties in 1 to $\sim$ 200nm films [23]. Since the time scale sensitivity of the μSR technique matches well the spin dynamics of SMMs [24, 25, 26], LE-μSR provides a perfect tool for studies of spin dynamics in thin film SMMs and the effect of the substrate on them. The depth resolved capability enables one to follow these gradually from the SMM/substrate interface to the surface of the film. However, in order to interpret results of such experiments, it becomes important to take into account effects of the substrate and the resulting SMM packing/configuration of the film.

In this paper, we present simulations of the dipolar field distribution acting on a single SMM, produced by its neighbours. We calculate the variation in the distribution as a function of the packing of SMMs and their proximity to the substrate, and discuss their effect on the molecular spin dynamics. Note that due to the strong correlation between the geometric SMM structure and its magnetic easy axis orientation, a change in the packing of molecules could drastically change the dipolar field distribution. As a guiding example, we take thin films of $TbPc_2$,

a prototypical SMM, where a competition between molecule-molecule and molecule-substrate interactions results in a clear variation of the SMM packing as a function of proximity to the SMM/substrate interface [27]. In these films the easy axis orientation of the $TbPc_2$ changes from pointing out of plane near the interface to in plane away from it. Our dipolar field calculations show that a lower fluctuation rate is expected in the region near the substrate, while enhanced dynamics are expected far away from it. This difference is mainly due to the local magnetic field distribution along and perpendicular to the easy axis of the SMM, which in turn influence the probability of transition between spin states due to mixing. We point out here that SMMs may be influenced by other factors as well, which we do not consider here. However, we expect that the ability to control the packing of SMMs in thin films, e.g. by changing the substrate material, may open a new avenue for controlling and tuning their spin dynamics.

2. Simulations

In what follows, we consider the case of a film of $TbPc_2$ deposited on a gold substrate. Near the substrate the molecular easy axis points along the z-direction (normal to the substrate) due to interactions with the substrate (Fig. 1, scenario **I**) [27]. Away from the substrate, where intermolecular interactions dominate, the easy axes of the molecules are randomly oriented within the xy plane (Fig. 1, scenario **II**). We calculate the dipolar magnetic field distributions, acting on a single SMM in the layer, along and perpendicular to its easy axis for both scenarios. For these calculations we assume that the SMMs are arranged in a two-dimensional square or triangular lattices, both with a lattice constant a and a magnetic moment per molecule of $\boldsymbol{\mu} = g\mu_B\mathbf{S}$. We also discuss the effect of random disorder in the layer on the field distribution.

Generally, for SMMs with a total ground spin state S and easy axis along z, the two spin ground states $|S, S_z\rangle = |S, \pm S\rangle$ are degenerate in zero applied magnetic field. In order to simulate this degeneracy, each molecule is randomly assigned a spin value $S_z = +S$ or $-S$, i.e. we assume a very low temperature limit, $T \to 0$. Since different spin values and orientation lead to different magnetic fields, we average the magnetic fields, $\mathbf{B}$, for different SMM configurations for each scenario.

The dipolar magnetic field of one SMM moment $\boldsymbol{\mu}_i$ produced on another amounts to,

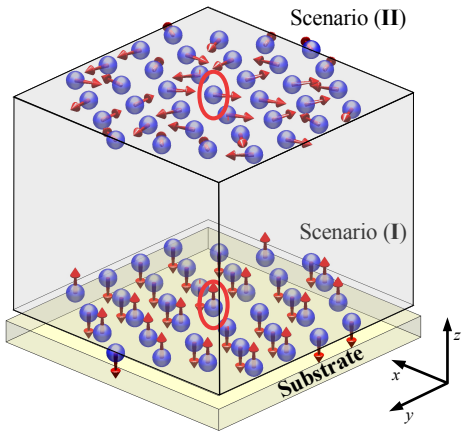

Figure 1. Illustration of two different scenarios for SMM packing, these are similar to the case of $TbPc_2$ thin films. The dipolar fields are calculated at the site of the marked SMM.

$$\mathbf{B}_i(\mathbf{r}_i) = \frac{\mu_0}{4\pi}\frac{3\mathbf{r}_i(\boldsymbol{\mu}_i \cdot \mathbf{r}_i) - \boldsymbol{\mu}_i r_i^2}{r_i^5}, \tag{1}$$

where $\mathbf{r}_i$ is the spacing vector between them. The resulting field of all contributing moments on a single SMM can be obtained by summing the fields of the individual moments. It is sufficient to take into consideration only a few neighbouring moments within a distance ρ from it [28]. Typically, the calculated field distribution converges for $\rho = 5a$. Note that here, since the average magnetization per unit area is zero in both scenarios, the contribution of moments outside ρ is zero [28]. For all the calculations performed here we use $|\boldsymbol{\mu}| = 1\mu_B$ ($S = 1/2$) with all distances normalized by a in Å units, giving the normalized dipolar fields in units of Å^{3}T (to be divided by a^3 to obtain the actual field).

3. Results

3.1. Near the substrate

We start by considering a layer of molecules which lie directly on the substrate. Assuming their easy axis (along z) is normal of the surface, the magnetic moment has only a component along the z-direction. Therefore, the magnetic field these molecules produce on an individual molecule in the same layer (highlighted red in Fig. 1) does not have components perpendicular to its easy axis. The results of the calculation described above for a triangular and a square lattice are shown in Fig. 2(a) and (b), respectively. In what follows, we distinguish between field

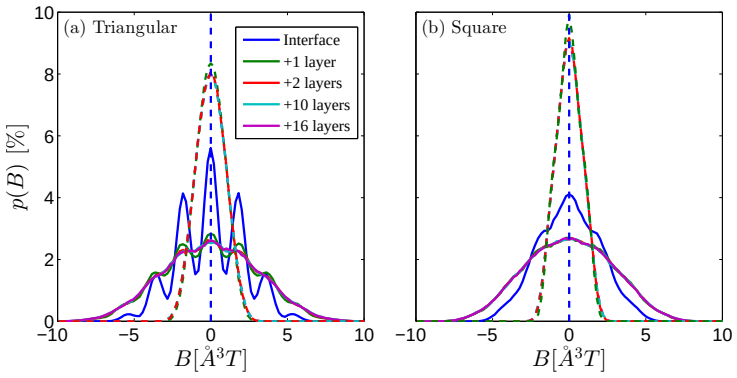

Figure 2. The dipolar field distribution calculated for scenario **I**, in the case of a (a) triangular and (b) square lattice. The solid and dashed lines represent $B_{\parallel}$ and $B_{\perp}$, respectively.

components along the SMM easy axis ($B_{\parallel}$) and perpendicular to it ($B_{\perp}$). Note, for both lattices, the probability for zero field is large. In the triangular lattice, there are also notable peaks at magnetic fields of $B_{\parallel} = 2n\beta$ Å^{3}T (where $\beta = \mu_0\mu_B/4\pi a^3$ and $n = 0,\ \pm1,\ \pm2$ and ±3). These are due to the six nearest neighbours and all their possible spin up/down configurations. For example, the zero field is experienced if three spins are assigned $S_z = +S$ and three are assigned $-S$. The probability for $B = 0$ reflects the number of possible configurations of three spins up and three down, i.e. $p(B = 0) = \binom{6}{3}(\sum_{k=0}^{6}\binom{6}{k})^{-1} = 31.25\%$. Magnetic moments further away, will broaden the distribution and a finite probability for intermediate magnetic fields emerge. In contrast, in the square lattice, each SMM has four nearest neighbours, but also four next-nearest neighbours with only slightly bigger distance. Therefore, the maxima are expected at $B_{\parallel} = 2n\beta$ (with $n = 0,\ \pm1$ and ±2). However, the strong contribution of the next-nearest neighbours produces high probability for intermediate fields as well.

Additional contributions from molecules lying above this first layer also contribute to the magnetic field distribution. Taking these into account produces some broadening of the probability distribution as shown in Fig. 2. Only the first two layers have a visible effect on the calculated field distribution. This is due to the $\frac{1}{r^3}$ dependence of the dipolar field. More importantly, the contribution of additional layers broadens the distributions of both $B_{\parallel}$ and $B_{\perp}$ components, as shown in Fig. 2. Here we assumed that the layers of molecules stack directly on top of each other with spacing a between them. However, different stacking will not change our general conclusions.

3.2. Far from the substrate

Next we consider a layer of molecules far away from the substrate, where we assume, as in the case of $TbPc_2$, that their easy axis is randomly oriented in the plane. We calculate the magnetic field distribution on an individual SMM, highlighted red in Fig. 1. Since the easy axes of the molecules are not parallel to one another, the produced dipolar magnetic fields

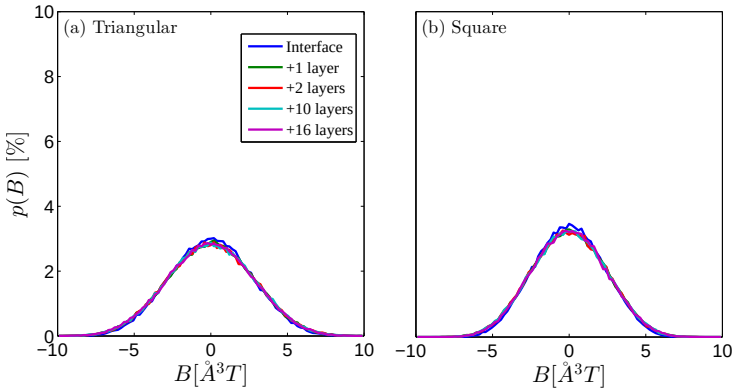

Figure 3. The dipolar field distribution calculated for scenario **II**, in the case of a (a) triangular and (b) square lattice. $B_\perp$ and $B_\parallel$ components are identical.

may point in random directions. Therefore, the probability for one molecule to experience magnetic field components perpendicular to its own easy axis is larger compared to scenario **I**. Moreover, the distributions of both $B_\parallel$ and $B_\perp$ are identical (Fig. 3). The distributions for both components/lattices are almost Gaussian and featureless since the moments are randomly aligned in the plane. It also remains unchanged when neighbouring layers are also considered.

3.3. Random lattice

The above calculations are based on the assumption of SMMs which are ordered on a regular lattice. In reality, the arrangement can be highly disordered in SMM thin films, especially far from the substrate. To take this into consideration, we introduce as small ($< a$) and random displacement of all SMMs from their lattice sites along the x and y directions,

$$\begin{aligned} x &\mapsto x + R\cos(\phi) \\ y &\mapsto y + R\sin(\phi). \end{aligned} \qquad (2)$$

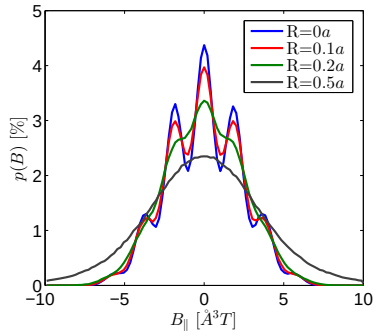

Figure 4. The effect of lattice randomization on $B_\parallel$ distribution calculated for scenario **I**.

Here, x and y denote the coordinates of a lattice site, R is random (uniform distribution) displacement magnitude and ϕ a random angle $\in (0, 2\pi)$ which determines the direction of the displacement. In Fig. 4, we plot as an example the magnetic field distribution, $B_\parallel$, calculated for a triangular lattice in scenario **I** for various values of R. In fact, the effect of disorder is almost equivalent to a convolution of the ordered lattice distribution with a function that mimics the randomization of the lattice,

$$f(B) = \begin{cases} 1 & |B| \leq \beta \left(\frac{R}{a}\right)^3 \\ 0 & \text{otherwise} \end{cases} \qquad (3)$$

The features, due to the nearest neighbours, mentioned above gradually disappear for larger R. We point out here that other random (non-uniform) displacements will naturally result in a different form of $f(B)$, e.g. a Gaussian distribution leads to a $f(B)$ with a Gaussian form, etc..

4. Discussion

In first approximation, the Hamiltonian of a magnetic molecule with easy axis along z is given by

$$\mathcal{H} = -DS_z^2 + g\mu_B \mathbf{B} \cdot \mathbf{S}, \tag{4}$$

where D is the axial anisotropy, S_z the spin operator along the easy axis and $\mathbf{B}$, $\mathbf{S}$ are the field and spin vector operators, respectively. In zero field (ZF), the eigenstates are $|S, M_S\rangle$, where S denotes the total spin quantum number and M_S is the azimuthal spin quantum number ($-S \leq M_S \leq S$). In the absence of magnetic fields, the ground state is twofold degenerate, $E(M_S = \pm S) = -DM_S^2$. If a field $\mathbf{B} = B\hat{z}$ is applied along the easy axis, then the energy levels of the spin states are $E(M_S) = -DM_S^2 \pm g\mu_B B M_S$, with the same eigenvectors as in the ZF case. However, the ground state degeneracy is removed and quantum tunnelling is prohibited, i.e. no transition between different spin states is possible. In contrast, a field applied perpendicular to the easy axis causes a change (mixing) of eigenstates. For example, if the magnetic field $\mathbf{B} = B\hat{x}$, then the Hamiltonian can be written as

$$\mathcal{H} = -D{S_z}^2 + g\mu_B B S_x = -D{S_z}^2 + \frac{g\mu_B}{2} B(S_+ + S_-) \tag{5}$$

where S_+ and S_- are the raising and lowering operators, $S_\pm = S_x \pm iS_y$. Consequently, the eigenstates are a mixture of states with different quantum spin numbers M_S. The first order mixing can be calculated using first order perturbation theory. A system, which is initially prepared in the ZF ground spin state, $\Psi_{gs} = \frac{1}{\sqrt{2}}(|S, S\rangle + |S, -S\rangle)$, has a finite probability for a transition to the first excited states, $\Psi_1 = \frac{1}{\sqrt{2}}(|S, S-1\rangle + |S, -S+1\rangle)$,

$$p(\Psi_{gs} \to \Psi_1) = \frac{{\mu_B}^2 B^2 S}{4D^2(2S-1)^2} \tag{6}$$

which can be understood as an enhancement in the spin dynamics.

From these simple quantum mechanical considerations, we expect that fields along the easy axis reduce tunnelling and slow spin dynamics at low temperatures, while fields perpendicular to it enhance spin dynamics. With this in mind, we compare spin dynamics in the two scenarios **I** and **II**. In scenario **I**, high probability for non-zero $B_\parallel$ is observed, while the distribution of $B_\perp$ is narrow (it fits to a Gaussian of width $\sigma \sim 2.509 \mathring{A}^3 T$). On the other hand, in scenario **II** the distribution of both, $B_\parallel$ and $B_\perp$ are identical with a Gaussian of width $\sigma \sim 6.799 \mathring{A}^3 T$. Note, the width of $B_\parallel$ in scenario **II** is smaller than **I**, while the width of $B_\perp$ is larger. Therefore, the spin dynamics in scenario **I** should be slower than that in **II**. Finally, we note that these general conclusions do not change with the type of lattice or the amount of random disorder. This is due to the fact that the field distribution is primarily affected by the relative orientation of the neighbouring spins rather than their geometric configuration.

5. Conclusion

In conclusion, we have modelled the dipolar field distribution experienced by an individual SMM along and perpendicular to its easy axis. We have also investigated the dependence of the calculated distribution on the arrangement of the SMMs in thin films. We find that different molecular configuration could alter significantly the molecular spin fluctuation rate of the SMM, due to the change in distribution of dipolar fields. Assuming a system similar to $TbPc_2$, where the packing changes as a function of proximity to the substrate, we expect the spin dynamics to change as a function of depth. In particular, the dynamics are slower in the layers near the substrate interface, but they are enhanced gradually as the SMMs are further away from it. These results point to a potential tweaking mechanism for tuning SMM spin dynamics by

manipulating the packing of SMMs in a thin film, e.g. by the choice of a substrate. We expect that such consideration could provide a new avenue for the design of new tunable SMM nanostructures. Finally, it is important to point out here that in these calculations we consider only dipolar interactions with neighbouring SMMs. In practice, however, other interactions of SMMs with their environment may be present, and may lead to different effects on spin dynamics. In fact, recent LE-μSR measurements on thin films of $TbPc_2$ have revealed an opposite substrate proximity effect to what is expected from dipolar interactions alone [29]. This is due to the special case of $TbPc_2$, which has an unpaired electron on its organic shell which introduces additional interactions between the SMMs themselves as well as the substrate.

References

[1] Gatteschi D, Sessoli R and Villain J 2006 *Molecular Nanomagnets* (Oxford University Press)
[2] Wernsdorfer W, Aliaga-Alcalde N, Hendrickson D N and Christou G 2002 *Nature* **416** 406–409
[3] Gatteschi D and Sessoli R 2003 *Angew. Chem. Int. Ed.* **42** 268
[4] Leuenberger M N and Loss D 2001 *Nature* **410** 789–793
[5] Tejada J, Chudnovsky E M, del Barco E, Hernandez J M and Spiller T P 2001 *Nanotechnology* **12** 181
[6] Ardavan A, Rival O, Morton J J L, Blundell S J, Tyryshkin A M, Timco G A and Winpenny R E P 2007 *Phys. Rev. Lett.* **98** 057201
[7] Naitabdi A, Bucher J P, Gerbier P, Rabu P and Drillon M 2005 *Adv. Mater.* **17** 1612
[8] Gomez-Segura J, Diez-Perez I, Ishikawa N, Nakano M, Veciana J and Ruiz-Molina D 2006 *Chem. Comm.* 2866–2868
[9] Burgert M, Voss S, Herr S, Fonin M, Groth U and Rudiger U 2007 *J. Am. Chem. Soc.* **129** 14362–14366
[10] Moroni R, Buzio R, Chincarini A, Valbusa U, de Mongeot F B, Bogani L, Caneschi A, Sessoli R, Cavigli L and Gurioli M 2008 *J. Mater. Chem.* **18**(1) 109–115
[11] Margheriti L *et al* 2009 *Small* **5** 1460–1466
[12] Mannini M *at al* 2009 *Nature Mater.* **8** 194–197
[13] Cavallini M, Facchini M, Albonetti C and Biscarini F 2008 *Phys. Chem. Chem. Phys.* **10**(6) 784–793
[14] Cornia A *et al* 2003 *Angew. Chem. Int. Ed.* **42** 1645
[15] Condorelli G G, Motta A, Fragalà I L, Giannazzo F, Raineri V, Caneschi A and Gatteschi D 2004 *Angew. Chem. Int. Ed.* **43** 4081
[16] Coronado E, Forment-Aliaga A, Romero F M, Corradini V, Biagi R, Renzi V D, Gambardella A and del Pennino U 2005 *Inorg. Chem.* **44** 7693–7695
[17] Fleury B, Catala L, Huc V, David C, Zhong W Z, Jegou P, Baraton L, Palacin S, Albouy P A and Mallah T 2005 *Chem. Commun.* 2020
[18] Salman Z *et al* 2007 *Nano Lett.* **7** 1551
[19] Mannini M *et al* 2010 *Nature* **468** 417–421
[20] Morenzoni E, Kottmann F, Maden D, Matthias B, Meyberg M, Prokscha T, Wutzke T and Zimmermann U 1994 *Phys. Rev. Lett.* **72** 2793
[21] Prokscha T, Morenzoni E, Deiters K, Foroughi F, George D, Kobler R, Suter A and Vrankovic V 2008 *Nucl. Instr. and Meth. A* **595** 317–331
[22] Morenzoni E, Glucker H, Prokscha T, Khasanov R, Luetkens H, Birke M, Forgan E M, Niedermayer C and Pleines M 2002 *Nuc. Inst. Meth. Phys.* **192** 254
[23] Morenzoni E, Prokscha T, Suter A, Luetkens H and Khasanov R 2004 *J. Phys.: Condens. Matter* **16** S4583–S4601
[24] Lascialfari A, Jang Z H, Borsa F, Carretta P and Gatteschi D 1998 *Phys. Rev. Lett.* **81** 3773
[25] Branzoli F, Carretta P, Filibian M, Graf M J, Klyatskaya S, Ruben M, Coneri F and Dhakal P 2010 *Phys. Rev. B* **82** 134401
[26] Salman Z, Giblin S R, Lan Y, Powell A K, Scheuermann R, Tingle R and Sessoli R 2010 *Phys. Rev. B* **82** 174427
[27] Margheriti L *et al* 2010 *Adv. Mater* **22** 5488–5493
[28] Salman Z and Blundell S 2012 *Physics Procedia* **30** 168–173
[29] Hofmann A, Salman Z, Mannini M, Amato A, Malavolti L, Morenzoni E, Prokscha T, Sessoli R and Suter A 2012 *ACS Nano* **6** 8390–8396